Quantifying the temperature-independent effect of stratospheric aerosol geoengineering on global-mean precipitation in a multi-model ensemble

A J Ferraro[1] and H G Griffiths[2]

[1] College of Engineering, Mathematics and Physical Sciences, University of Exeter, Exeter, Devon, UK

[2] School of Geographical Sciences, University of Bristol, Bristol, UK

E-mail: a.j.ferraro@exeter.ac.uk

Abstract. The reduction in global-mean precipitation when stratospheric aerosol geoengineering is used to counterbalance global warming from increasing carbon dioxide concentrations has been mainly attributed to the temperature-independent effect of carbon dioxide on atmospheric radiative cooling. We demonstrate here that stratospheric sulphate aerosol itself also acts to reduce global-mean precipitation independent of its effects on temperature. The temperature-independent effect of stratospheric aerosol geoenginering on global-mean precipitation is calculated by removing temperature-dependent effects from climate model simulations of the Geoengineering Model Intercomparison Project (GeoMIP). When sulphate aerosol is injected into the stratosphere at a rate of 5 Tg SO_2 per year the aerosol reduces global-mean precipitation by approximately 0.2 %, though multiple ensemble members are required to separate this effect from internal variability. For comparison, the precipitation reduction from the temperature-independent effect of increasing carbon dioxide concentrations under the RCP4.5 scenario of the future is approximately 0.5 %. The temperature-independent effect of stratospheric sulphate aerosol arises from the aerosol's effect on tropospheric radiative cooling. Radiative transfer calculations show this is mainly due to increasing downward emission of infrared radiation by the aerosol, but there is also a contribution from the stratospheric warming the aerosol causes. Our results suggest climate model simulations of solar dimming can capture the main features of the global-mean precipitation response to stratospheric aerosol geoengineering.

precipitation, radiative forcing, geoengineering, climate engineering, climate modelling, GeoMIP

Submitted to: *Environ. Res. Lett.*

1. Introduction

As global warming from anthropogenic greenhouse gas emissions continues, it has been proposed that scientists investigate the potential of using stratospheric aerosol geoengineering to offset some of the warming (Crutzen 2006, Wigley 2006, Keith et al. 2010). Injection of sulphate into the stratosphere might be technically feasible (Robock et al. 2009, McClellan et al. 2012, Davidson et al. 2012) but it poses substantial risks. For example, using it to counterbalance the warming from increasing carbon dioxide (CO_2) concentrations would reduce global-mean precipitation (Govindasamy & Caldeira 2000, Bala et al. 2008, Schmidt et al. 2012, Tilmes et al. 2013).

Changes in the global-mean precipitation rate are balanced by changes in the rate at which the atmosphere can radiate the latent heat released by condensation of water vapour (Allen & Ingram 2002, Lambert & Webb 2008, Andrews et al. 2009, Pendergrass & Hartmann 2014). Since a warmer atmosphere emits more infrared radiation, atmospheric radiative cooling increases with surface warming. Climate models indicate radiative cooling increases at a rate of approximately 2% per Kelvin of global-mean surface warming, increasing precipitation by a similar amount. Changes in atmospheric radiative cooling could also be balanced by changes in surface sensible heat flux, but in both observations and climate model simulations this contribution is smaller than that from the latent heat flux (O'Gorman et al. 2012).

CO_2 and other radiatively active species can also directly influence atmospheric radiative cooling, independent of temperature. Greenhouse gases reduce this cooling rate and consequently reduce global-mean precipitation. An abrupt increase in CO_2 concentrations produces a rapid decrease in global-mean precipitation as the temperature-independent effect of the CO_2 acts almost instantaneously, but as the surface warms the net effect is an increase in precipitation relative to an unperturbed state (Mitchell et al. 1987, Lambert & Webb 2008). If geoengineering is used to reduce global-mean surface temperature without removing CO_2, the temperature-dependent increase in precipitation will be removed but the temperature-independent decrease from the temperature-independent effect of CO_2 will remain, resulting in a net reduction in precipitation (Bala et al. 2008, Kleidon & Renner 2013).

The global-mean precipitation response to increasing CO_2 concentrations can be expressed as:

$$L\Delta P = a\Delta T + bF_{CO_2} \tag{1}$$

where L is the latent heat of condensation of water, ΔP is the change in global-mean precipitation rate, ΔT is the global-mean temperature change and F_{CO_2} is the radiative forcing at the top of the atmosphere associated with CO_2 changes. The constants a and b are the sensitivity of global-mean atmospheric radiative cooling to surface temperature change and CO_2 radiative forcing respectively. In our formulation we assume all sensible heat flux changes are driven by surface temperature changes so they can be subsumed into a. The coefficient a can be converted to a 'hydrological

sensitivity' describing the response of precipitation to surface temperature change by dividing by the latent heat of condensation of water. Climate models simulations give a fractional hydrological sensitivity of approximately 2 % K^{-1} (Thorpe & Andrews 2014). The value of b depends primarily on the vertical profile of the radiative forcing. It can be expressed as the fraction of the radiative forcing absorbed by the atmosphere:

$$b = \frac{F_s - F}{F} \tag{2}$$

where F_s is the surface radiative forcing. A forcing agent which has a constant vertical profile of radiative forcing would have $b = 0$ and no effect on global-mean precipitation because this implies none of the forcing is absorbed by the atmosphere. For CO_2, b has been estimated to be between -0.8 by Andrews et al. (2010) and -0.6 by Kvalevåg et al. (2013).

Niemeier et al. (2013) demonstrated that stratospheric aerosols themselves can change global-mean precipitation by increasing downward emission of infrared radiation from the stratosphere into the troposphere. Ferraro et al. (2014) investigated the mechanism by which the 'greenhouse effect' of stratospheric sulphate can influence tropical precipitation using idealised climate model simulations with a large aerosol loading placed directly above the tropopause. The additional downward infrared emission was absorbed in the troposphere, increasing static stability and weakening convective vertical motion. This work suggested the temperature-independent effect of stratospheric aerosols on tropical precipitation could be of comparable magnitude to the temperature-independent effect of CO_2.

However, Ferraro et al. (2014) used very large mass loadings of stratospheric aerosol directly above the tropical tropopause. It is not clear what a realistic altitude, mass loading and size distribution of a geoengineering sulphate aerosol layer might be; climate models produce different aerosol layer altitudes and mass loadings in response to large injections of sulphur dioxide (Pitari et al. 2014). It is therefore important to quantify the importance of this mechanism in more moderate geoengineering scenarios across a range of different climate models. Niemeier et al. (2013) investigated this effect in simulations with the MPI-ESM-LR climate model in which care had to be taken to remove as much as possible the effects of surface temperature changes through careful prescription of the geoengineering forcing and additional bias correction based on the residual top-of-atmosphere radiative imbalance. They compared a simulation in which the positive radiative forcing during the 21st Century in the RCP4.5 scenario (Moss et al. 2010) was counterbalanced either using stratospheric aerosol injection or by reducing total solar irradiance. They showed a temperature-independent precipitation reduction associated with the aerosol of approximately 0.3% (0.009 mm day^{-1}) during the period 2060-2069. For comparison, the precipitation reduction from the temperature-independent effect of CO_2 (calculated as the difference between the simulation with reduced solar irradiance and a simulation with fixed CO_2 concentrations) was 0.5% (0.014 mm day^{-1}). Thus the additional precipitation decline associated with the temperature-independent effect of sulphate was approximately two thirds that of CO_2.

The analysis of Niemeier et al. (2013) required that differences in surface temperature between the simulations were minimised in order to quantify the temperature-independent components. However, many simulations of stratospheric aerosol geoengineering conducted under the Geoengineering Model Intercomparison Project (GeoMIP) have large residual temperature changes. Thus, the precipitation changes from different models have different temperature-dependent components, making it difficult to readily analyse the temperature-independent effect in a multi-model framework. This paper uses an energetic framework to remove the effects of these temperature changes in order to estimate the temperature-independent effect of stratospheric sulphate geoengineering aerosol on global-mean precipitation. We investigate the detectability of the temperature-independent effect and the sources of differences in its magnitude among models.

2. Methods

GeoMIP includes a number of scenarios in which the radiative forcings in the RCP4.5 scenario of the future are combined with geoengineering using solar dimming or stratospheric aerosols. The GeoMIP scenarios differ from RCP4.5 in terms of radiative forcing and surface temperature. By removing the temperature-dependent component of precipitation change from RCP4.5 and the geoengineering simulations, any remaining differences in global-mean precipitation will be attributable to the geoengineering forcing.

We modify the conventional framework for analysing temperature-dependent and temperature-independent changes in precipitation by adding a term representing a hypothesised temperature-independent effect of stratospheric sulphate aerosol:

$$L\Delta P = a\Delta T + b_{RCP}F_{RCP} + b_{GE}F_{GE} \tag{3}$$

The first term on the right-hand side of Equation 3 is the temperature-dependent term. If we assume that the coefficient a is not dependent on temperature or forcing agent, the same a can be used to remove the temperature-dependent component of precipitation change from any model simulation. The second term on the right-hand side of Equation 3 is the temperature-independent term associated with non-geoengineering forcings. This is primarily due to increasing CO_2 concentrations from anthropogenic sources, but also includes other anthropogenic greenhouse gases and tropospheric aerosols. In this paper we use model projections for the 21st Century following RCP4.5, so we use F_{RCP} to denote the forcing from non-geoengineering sources and b_{RCP} to denote the fraction of this forcing that is absorbed by the atmosphere. The third and final term on the right-hand side of Equation 3 represents the hypothesised temperature-independent effect on the geoengineering forcing. F_{GE} denotes the geoengineering forcing and b_{GE} denotes the fraction of this forcing that is absorbed by the atmosphere.

We estimate the coefficient a by regressing annual-mean precipitation change following an abrupt quadrupling of atmospheric CO_2 concentrations against the

Table 1. Climate models used in this study. 'HS' denotes the hydrological sensitivity, which is calculated by dividing a by the latent heat of condensation of water and converted to a fractional change by dividing by climatological precipitation. Uncertainties on HS are two standard errors from the ordinary least squares regression. The 'RCP4.5', 'G3', 'G3S' and 'G4' columns give the number of ensemble members from each simulation used in the analysis.

Model	HS (% K^{-1})	RCP4.5	G3	G3S	G4	Reference
CanESM2	2.51 ± 0.07	5	-	-	3	von Salzen et al. (2013)
HadGEM2-ES	2.10 ± 0.05	4	3	3	3	Martin et al. (2011)
MPI-ESM-LR	2.54 ± 0.07	4	3	-	-	Stevens et al. (2013)

corresponding temperature change, as done by, for example, Lambert & Webb (2008) and Andrews et al. (2009). This is done by calculating changes in the 'abrupt4xCO2' CMIP5 simulations relative to the 'piControl' (pre-industrial control) simulations of each model. The slope of the regression line gives the sensitivity of global-mean precipitation to changes in global-mean surface temperature, which we call the hydrological sensitivity, and the intercept of the line gives the temperature-independent effect of CO_2. The estimated values for the hydrological sensitivity are given in Table 1.

We analyse output from the G3, G3S and G4 GeoMIP simulations. The G3 and G3S simulations aim to offset the radiative forcing from RCP4.5 over the years 2020-2070, though residual temperature changes often remain (Berdahl et al. 2014) which will be accounted for using our method (Equation 3). The G3 simulations use stratospheric sulphate aerosol, whereas the G3S simulations use a reduction in total solar irradiance to represent geoengineering. The G4 simulations use constant stratospheric sulphate injection corresponding to 5 Tg SO_2 per year. Thus, the geoengineering forcing remains constant in time in the G4 scenario, but increases with time in G3 and G3S. We calculate changes in temperature and precipitation between 2020 and 2070 relative to the 2006-2015 climatology from RCP4.5.

Our analysis uses output from three climate models, listed together with the number of available ensemble members for each experiment in Table 1. Other models performed G3, G3S and G4 simulations, but are excluded because they were performed in different computational environments to their corresponding RCP4.5 simulations. Differences in computer hardware and software therefore prevent direct comparison of the RCP4.5 and GeoMIP simulations for BNU-ESM and GISS-E2-R. The IPSL-CM5A-LR model is excluded because it did not include the infrared effects of stratospheric sulphate aerosol in its radiative transfer calculations (O. Boucher, *pers. comm.*). The NorESM1-M model is excluded because of a bug in calculation of the infrared effects of stratospheric sulphate aerosol (J. E. Kristjansson, *pers. comm.*).

We also investigate the physical mechanisms of the temperature-independent effect of stratospheric sulphate aerosol using a broadband radiative transfer model, SOCRATES (Suite of Community Radiation Codes based on Edwards & Slingo (1996)).

This model is used as the radiative transfer component of the various configurations of the UK Met Office's Unified Model, including the HadGEM2 climate model (Martin et al. 2011), which we analyse in this paper. Radiative fluxes we calculate for HadGEM2 will therefore be internally consistent with our radiative transfer model; this will not be the case for other climate models we analyse. We calculate infrared radiative fluxes in nine spectral bands. Eight bands cover wavelengths between 3.3 and 25 μm, and the remaining band covers wavelengths between 25 μm and 1 cm. Sulphate aerosol absorption and extinction coefficients are calculated from refractive indices using Mie theory (Zdunkowski *et al* 2007), assuming the aerosol is composed of 75% sulphuric acid and 25% water and have an effective radius of 0.22 μm. This radius is representative of volcanic aerosol. It is likely that, if aerosol is continuously injected into the stratosphere, the particles could grow to larger radii (Heckendorn et al. 2009, Niemeier et al. 2011, English et al. 2012). Larger aerosols tend to absorb more longwave radiation for a given shortwave scattering, so our calculations of the tropospheric heating from downward emission of longwave radiation could be underestimates.

3. Results

3.1. Separating temperature-dependent and temperature-independent effects

Figure 1 shows the precipitation changes between 2006 and 2070 in the RCP4.5 and geoengineering simulations. Global-mean precipitation increases under RCP4.5. Precipitation changes in geoengineering simulations depend on the model and on the geoengineering scenario, but in all cases geoengineering reduces precipitation relative to RCP4.5. In order to calculate the temperature-independent component of these precipitation changes we must subtract the temperature-dependent component. The temperature-dependent component is calculated by multiplying the temperature change in each simulation (shown in Figure S1) by the model's hydrological sensitivity.

Figure 2 shows that there are substantial temperature-dependent precipitation changes in some of the geoengineering simulations. The MPI-ESM-LR G3 simulation successfully counterbalances the warming in RCP4.5, so it has very little temperature-dependent precipitation change (Figure 2c). On the other hand the G3 simulation of HadGEM2-ES shows non-negligible temperature-dependent precipitation changes, indicating there is some residual warming. There are also contrasting behaviours between the two models that performed the G4 experiment. In HadGEM2-ES (Figure 2b) the G4 forcing produces global cooling, driving a reduction in precipitation, between 2020 and 2040. There is no such cooling in CanESM2, indicating the models produce rather different surface temperature responses to stratospheric sulphate aerosol injection. This could arise for three reasons: differences in the in the specification of stratospheric sulphate aerosol, differences in the forcing resulting from the aerosol (Chung & Soden (2015) showed climate models do not calculate the same forcings even with identical changes in atmospheric composition), or differences in the models' responses to the

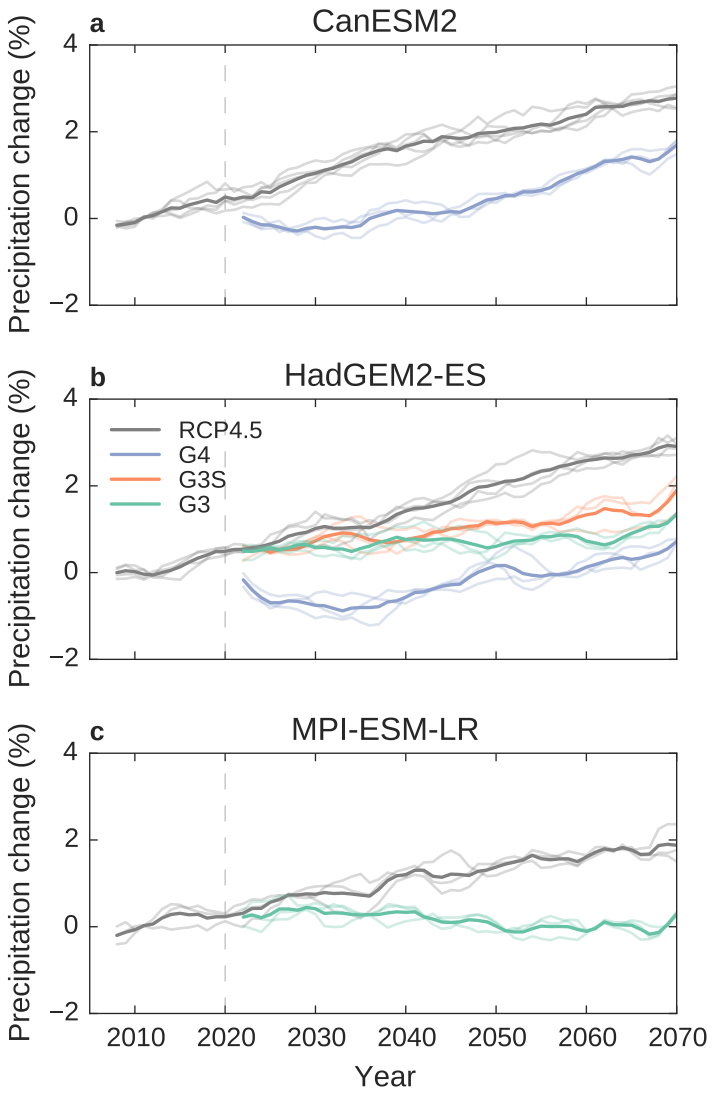

Figure 1. Precipitation changes. Annual-mean changes are calculated relative to the 2006-2015 climatology from RCP4.5 and smoothed with a 5-year running mean. Light lines show ensemble members and dark lines show averages over all available ensemble members. The vertical dashed grey line shows the year in which geoengineering begins.

forcing.

The temperature-independent component of precipitation change is calculated by subtracting the temperature-dependent component from the total precipitation change. The results are shown in Figure 3.

There is little difference in the temperature-independent precipitation change between G3S and RCP4.5 in HadGEM2-ES. This is as expected, since the effect of changing solar irradiance on net atmospheric radiative cooling is relatively small (**?**, Kvalevåg et al. 2013). Notably, there is no statistically significant difference between G3S and RCP4.5 even when ensemble-mean precipitation changes are used (Table 2).

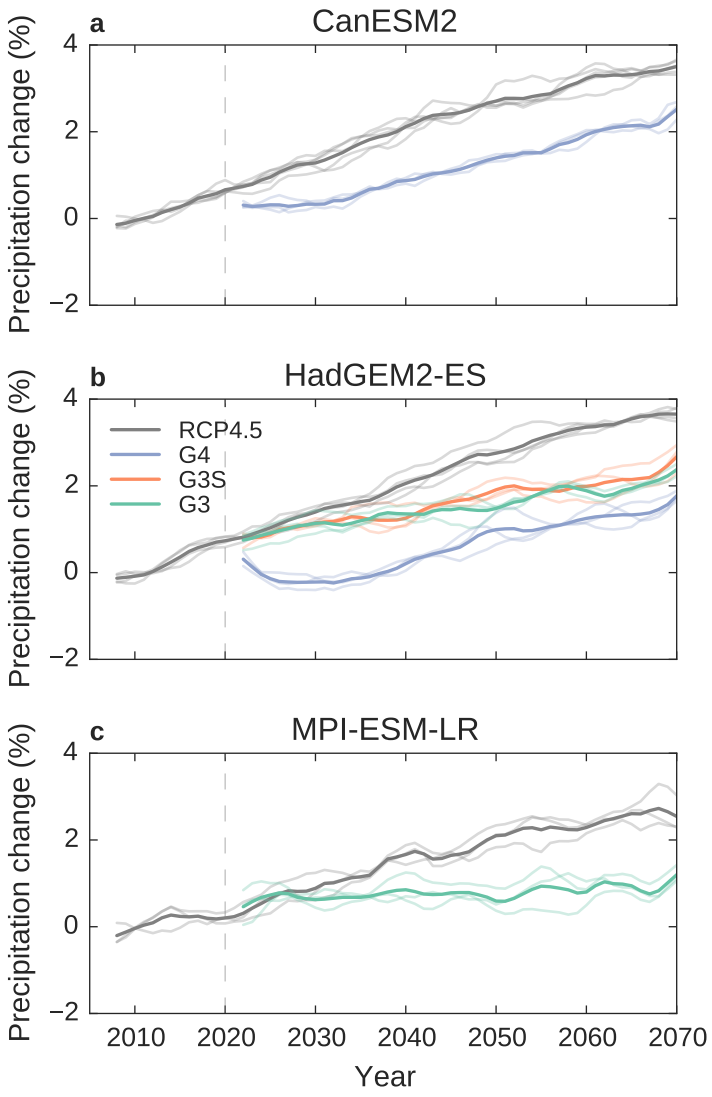

Figure 2. Temperature-dependent precipitation changes. Annual-mean changes are calculated relative to the 2006-2015 climatology from RCP4.5 and smoothed with a 5-year running mean. Light lines show ensemble members and dark lines show averages over all available ensemble members. The vertical dashed grey line shows the year in which geoengineering begins.

The G3 HadGEM2-ES simulation has a more negative temperature-independent component of precipitation change than RCP4.5. However, individual HadGEM2-ES G3 ensemble members do not. This shows the temperature-independent precipitation reduction is small compared with internal variability, indicating it is not major cause of precipitation changes in these simulations. The difference between the RCP4.5 and G3 ensemble means is especially apparent in the latter part of the simulation, which is as expected since this is when the G3 aerosol forcing is strongest. Similarly, MPI-ESM-LR shows a statistically significant temperature-independent precipitation

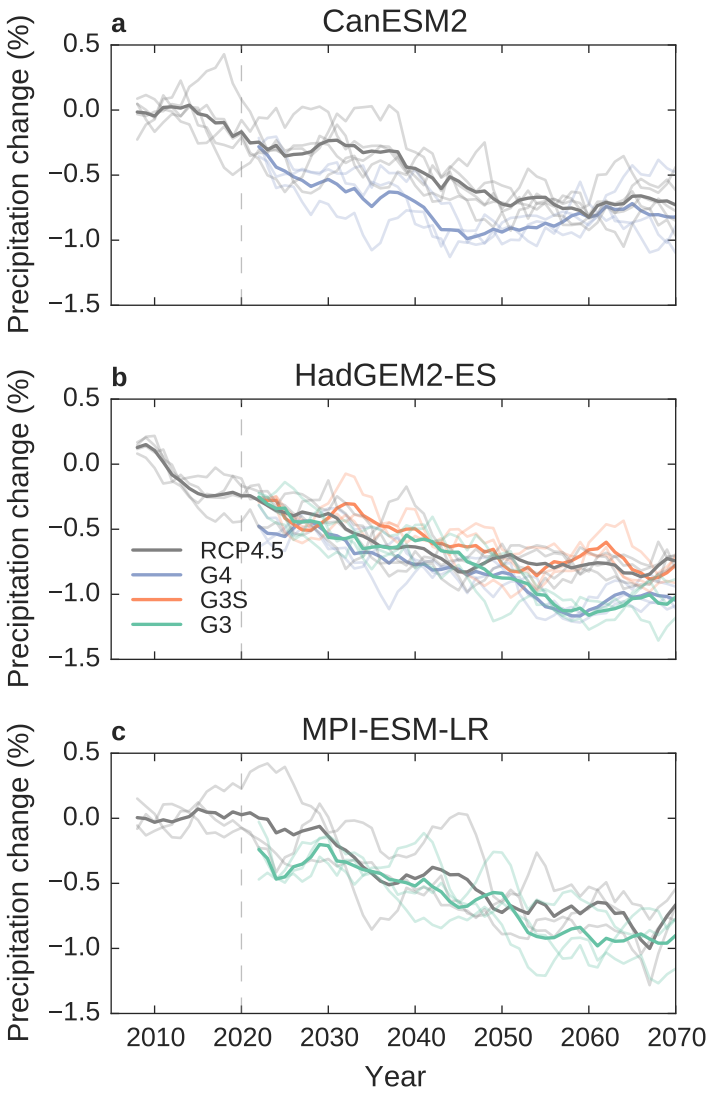

Figure 3. Temperature-independent precipitation changes. Annual-mean changes are calculated relative to the 2006-2015 climatology from RCP4.5 and smoothed with a 5-year running mean. Light lines show ensemble members and dark lines show averages over all available ensemble members. The vertical dashed grey line shows the year in which geoengineering begins.

decrease compared to RCP4.5 (Figure 3 and Table 2).

There are also large differences in the temperature-independent precipitation change in the G4 case. For HadGEM2-ES the temperature-independent precipitation reduction is greater than RCP4.5 for nearly the entire length of the simulation. For CanESM2 the effect of the aerosol is largest between 2020-2050, and very small between 2060-2070. This is unexpected since the geoengineering forcing is constant in time in G4. It is possible that the hydrological sensitivity in fact varies with time, and that in the CanESM2 simulations this time variation is non-negligible. Another

Table 2. Temperature-independent precipitation changes in RCP4.5 and geoengineering simulations averaged between 2020 and 2069. The final column contains p-values calculated using a two-tailed t test for difference between means of RCP4.5 and the geoengineering simulation, accounting for autocorrelation in the annual time-series.

Model	Simulation	RCP4.5 (%)	Geoengineering (%)	p-value for difference
CanESM2	G4	-0.52	-0.72	5.8×10^{-7}
HadGEM2-ES	G3	-0.64	-0.74	0.01
HadGEM2-ES	G3S	-0.64	-0.59	0.92
HadGEM2-ES	G4	-0.64	-0.80	1.80×10^{-7}
MPI-ESM-LR	G3	-0.48	-0.61	0.002

possible explanation is that additional temperature-independent effects not related to downward infrared emission from the stratosphere may be modifying precipitation. For example, Fyfe et al. (2013) showed that the increased CO_2 concentrations and moderate temperatures in geoengineering simulations reduces transpiration by vegetation, which acts to reduce global-mean precipitation. Repeating this analysis with additional CanESM2 ensemble members would indicate whether unforced internal variability can produce this effect or whether it is caused by some other mechanism, such as the vegetation response.

In spite of the potential confounding effects of internal climate variability, in the ensemble-mean there is a robust temperature-independent reduction in precipitation relative to RCP4.5. These changes are, however, much smaller than the temperature-independent decline in precipitation associated with the other forcings in the RCP4.5 scenario, dominated by CO_2 changes (Thorpe & Andrews 2014).

Our analysis depends on the estimation of the hydrological sensitivity from regression of precipitation changes against temperature changes following an abrupt quadrupling of CO_2. The regression slope is a sample statistic and therefore has an associated uncertainty. Table 1 shows the standard error on the hydrological sensitivity is at least an order of magnitude less than the hydrological sensitivity itself, indicating this uncertainty does not have a major effect on our diagnosis of the temperature-dependent and temperature-independent components of precipitation change. We can verify this by repeating our analysis with the hydrological sensitivity set to be two standard errors higher or lower than our central estimate. The resulting spread in temperature-independent precipitation changes are shown in Figure 4. The uncertainty in hydrological sensitivity cannot explain the differences in the temperature-independent precipitation changes in the aerosol geoengineering simulations and RCP4.5. Note, however, that CanESM2 has a larger spread in estimated temperature-independent precipitation change because its a has a relatively high uncertainty. This may partially account for the apparent decrease of the difference between RCP4.5 and G4 between 2050-2070.

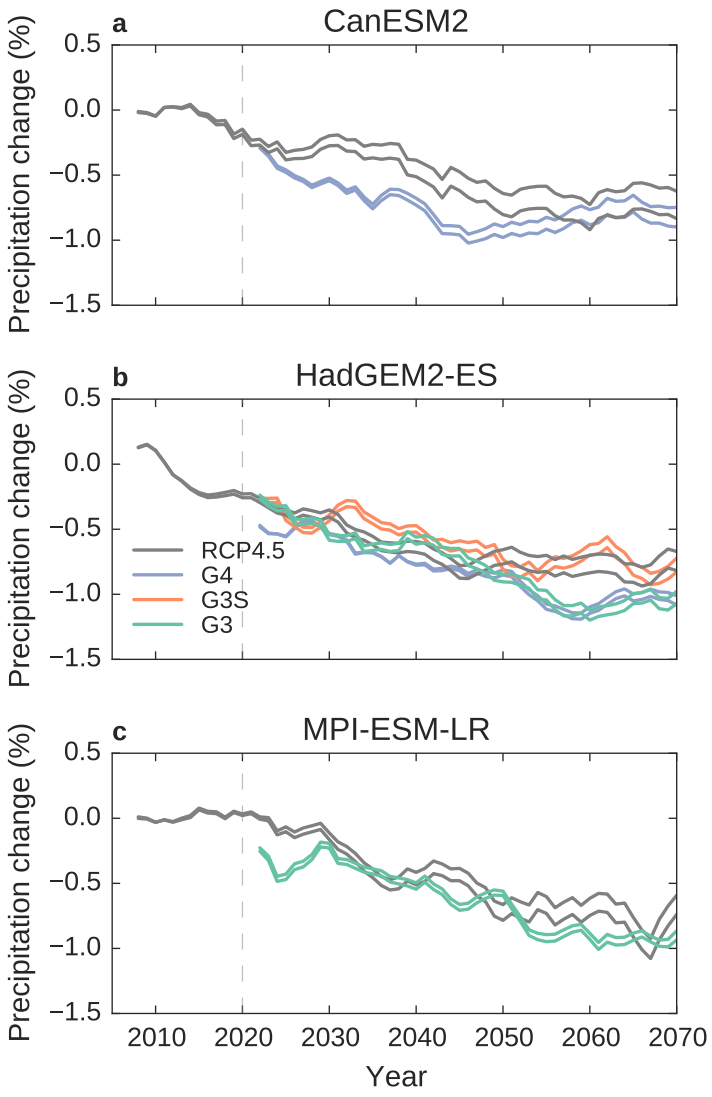

Figure 4. The effect of uncertainty in the regression-based estimate of a on temperature-independent precipitation change. Each simulation has two lines representing two standard errors either side of the best estimate of a. The vertical dashed grey line shows the year in which geoengineering begins.

3.2. Physical mechanisms of the temperature-independent effect

The temperature-independent effect of stratospheric sulphate aerosol on global-mean precipitation was explained by Niemeier et al. (2013) as being due to absorption and re-emission of infrared radiation by the aerosol. Niemeier et al. (2013) showed that this decrease in atmospheric radiative cooling from the aerosol's greenhouse effect is mainly balanced by changes in latent heating by precipitation. Here we quantify this effect in the four geoengineering simulations used in our analysis: G4 for CanESM, G3 and G4 for HadGEM2-ES and G3 for MPI-ESM-LR. We calculate radiative fluxes using the SOCRATES radiative transfer model. The calculation is

restricted to the infrared spectral region since changes in shortwave radiation have a relatively small effect temperature-independent effect on global-mean precipitation (this is demonstrated by negligible temperature-independent effect of the solar dimming in the HadGEM2-ES G3S simulation). We calculate radiative fluxes based on monthly climatologies 2020-2069 for RCP4.5, then perform additional calculations that include the stratospheric aerosol climatology from the relevant geoengineering simulation. The infrared absorption by the aerosol also drives stratospheric warming (Ferraro et al. 2011), which would increase downward emission of infrared radiation into the troposphere, so we perform a separate calculation including this effect. For the purposes of prescribing stratospheric temperature change we adopt a simplified tropopause definition: 100 hPa within 30 degrees of the Equator, 200 hPa between 30 and 60 degrees, and 300 hPa poleward of 60 degrees latitude.

These radiative transfer calculations are used to estimate changes in precipitation by calculating the change in tropospheric radiative heating (the difference between radiative flux at the surface and the tropopause) and dividing by the latent heat of condensation of water (2.5×10^6 J kg^{-1} K $^{-1}$). We focus on the troposphere rather than the whole atmospheric column since the latent heating by precipitation is almost entirely confined to the troposphere.

Figure 5 compares the simulated temperature-independent precipitation change over the geoengineering period with the effects of stratospheric temperature and aerosol on tropospheric radiative cooling calculated by SOCRATES. Stratospheric warming acts to decrease precipitation by decreasing tropospheric radiative cooling. The aerosol acts to decrease precipitation through its 'greenhouse effect'. The aerosol effect is much larger than the temperature effect. The sum of the two effects gives a precipitation reduction close to that simulated by the climate models. Differences between the precipitation changes predicted from the SOCRATES calculations and simulated by the models may be due to changes in sensible heat flux balancing some of the changes in radiative cooling (Niemeier et al. 2013). It may also be due to the idealised nature of the radiative transfer calculation - we use a time-constant basic state from RCP4.5, and neglect shortwave effects. Although our estimates are not identical to the simulated changes, these results demonstrate that the greenhouse effect of stratospheric aerosols is strong enough to have a substantial effect on precipitation through modification of the atmospheric energy balance, and that it is the aerosol greenhouse effect that dominates. However, a substantial part of the diversity of response between models and geoengineering scenarios comes from the effect of changing stratospheric temperatures. For example, the HadGEM2-ES G3 simulation has relatively little stratospheric warming and consequently a small effect of stratospheric temperature change on precipitation, whereas the MPI-ESM-LR G3 simulation has more stratospheric warming and an effect on precipitation approximately 3 times larger.

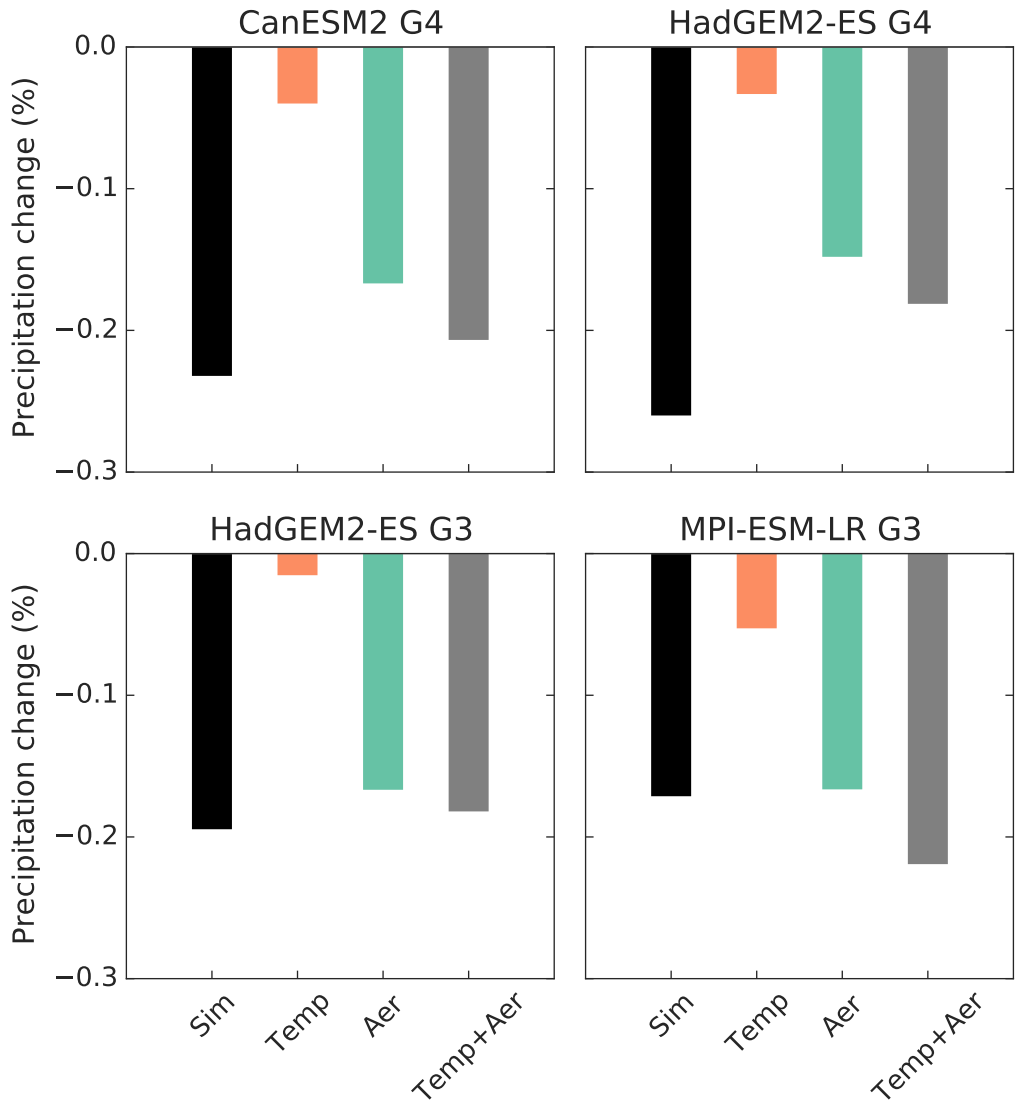

Figure 5. Comparison of simulated temperature-independent precipitation change to the change estimated based on radiative transfer calculations of tropospheric energy budget averaged over 2020-2069. 'Sim' (black bars) refers to the temperature-independent precipitation change simulated by the climate model. 'Temp' (orange bars) is the calculated effect of changing stratospheric temperature on tropospheric radiative cooling. 'Aer' (green bars) is the calculated effect of the tropospheric aerosol layer on atmospheric radiative cooling. 'Temp+Aer' (grey bars) is the combination of the temperature and aerosol effects.

4. Conclusions

After subtracting temperature-dependent precipitation changes, we have identified a temperature-independent effect on precipitation in stratospheric sulphate aerosol geoengineering simulations. We use the concept of hydrological sensitivity (the sensitivity of precipitation to surface temperature changes, which is assumed to be constant) to remove temperature-dependent precipitation changes. This allows us to analyse the temperature-independent precipitation changes associated with stratospheric aerosol geoengineering even in model simulations with substantial temperature trends.

When stratospheric sulphate aerosol is injected at a rate of 5 Tg SO_2 per year in the GeoMIP G4 simulations (giving a radiative forcing of approximately -1.2 Wm^{-2}) the additional temperature-independent effect is approximately -0.2%. Our analysis reveals there is substantial interannual and interdecadal variability in this value. The effect is only detectable when multiple realizations are available. Thus, multiple ensemble members and/or long time periods must be analysed to diagnose the temperature-independent effect of sulphate accurately. There are also other temperature-independent effects not driven by atmospheric radiative transfer, such as the reduction in transpiration by vegetation caused by increased CO_2 concentrations (Fyfe et al. 2013), that our analysis does not capture.

Iles & Hegerl (2014) showed that CMIP5 models underestimate the precipitation response to volcanism. Our framework could in principle be applied to identify whether this disagreement between models and observations arises more from temperature-dependent or temperature-independent effects. However, observational sample sizes are small since there are only a few volcanic eruptions in the observational record, which makes detection of the combined effect on precipitation difficult (Iles et al. 2013, Iles & Hegerl 2014). Such sampling uncertainty would also apply to decomposing the components of precipitation change.

Since multiple ensemble members are required to detect the temperature-independent effect, it is unlikely to present a major problem in a real-world application of geoengineering as simulated in the GeoMIP G3 and G4 scenarios. In these scenarios geoengineering forcings are comparable in magnitude to the radiative forcing in the RCP4.5 scenario of the future, i.e. 4.5 Wm^{-2}. Although larger forcings from stratospheric sulphate injection are theoretically possible (Niemeier & Timmreck 2015), this would suggest that stratospheric aerosol geoengineering over the range of forcings plausible for the 21st Century is unlikely to produce a significantly larger decrease in precipitation than a commensurate reduction in total solar irradiance. Thus, model simulations of solar dimming can provide useful information on the potential global-mean precipitation response to stratospheric aerosol geoengineering.

This does not preclude larger regional changes in precipitation, for example through a weakening of the tropical overturning (Ferraro et al. 2014) or shifts of the midlatitude jets (Ferraro et al. 2015). However, analyses by Niemeier et al. (2013) and Kalidindi et al.

(2014) do not reveal substantial differences in regional precipitation changes between geoengineering with stratospheric aerosols and solar dimming. This suggests that solar dimming simulations can capture much of the climate response to stratospheric aerosol geoengineering. The global and regional precipitation response appears to be sensitive to the altitude and spatial distribution of the aerosol layer and the size distribution of the particles (Kalidindi et al. 2014). This is important because the properties of the aerosol layer depend on modelling assumptions (Benduhn & Lawrence 2013, Pitari et al. 2014) and on the aerosol injection strategy. Finally, geoengineering using aerosols other than sulphate may have different climate impacts. For example, alumina and diamond aerosol produce less stratospheric heating and so will have a smaller effect on the tropospheric infrared heating (Weisenstein et al. 2015). Future work could investigate the sensitivity of the precipitation response to these assumptions to determine the importance of the radiative and dynamical effects of the aerosol for the climate response to geoengineering.

Acknowledgments

We thank Hugo Lambert and Mat Collins for useful discussions, and Ulrike Niemeier for extensive help with data access. A. Ferraro was supported by the Natural Environment Research Council PROBEC grant (NE/K016016/1). H. Griffiths was supported by the Engineering and Physical Sciences Research Council Vacation Bursary Scheme. We thank all the climate modelling groups for conducting the GeoMIP simulations and making their output available. We acknowledge the World Climate Research Programme's Working Group on Coupled Modelling, which is responsible for CMIP, and we thank the climate modelling groups (listed in Table 1 of this paper) for producing and making available their model output. For CMIP the U.S. Department of Energy's Program for Climate Model Diagnosis and Intercomparison provides coordinating support and led development of software infrastructure in partnership with the Global Organization for Earth System Science Portals.

References

Allen M R & Ingram W J 2002 *Nature* **419**(6903), 224–232.

Andrews T, Forster P M, Boucher O, Bellouin N & Jones A 2010 *Geophysical Research Letters* **37**(14), L14701.

Andrews T, Forster P M & Gregory J M 2009 *Journal of Climate* **22**(10), 2557–2570.

Bala G, Duffy P B & Taylor K E 2008 *Proceedings of the National Academy of Sciences of the United States of America* **105**(22), 7664–7669.

Benduhn F & Lawrence M G 2013 *Journal of Geophysical Research: Atmospheres* **118**(14), 7905–7921.

Berdahl M, Robock A, Ji D, Moore J C, Jones A, Kravitz B & Watanabe S 2014 *Journal of Geophysical Research: Atmospheres* **119**(3), 1308–1321.

Chung E S & Soden B J 2015 *Environmental Research Letters* **10**(7), 074004.

Crutzen P J 2006 'Albedo enhancement by stratospheric sulfur injections: A contribution to resolve a policy dilemma?'.

Davidson P, Burgoyne C, Hunt H & Causier M 2012 *Philosophical Transactions of the Royal Society A: Mathematical, Physical and Engineering Sciences* **370**(1974), 4263–4300.

Edwards J M & Slingo A 1996 *Quarterly Journal of the Royal Meteorological Society* **122**, 689–719.

English J M, Toon O B & Mills M J 2012 *Atmospheric Chemistry and Physics* **12**(10), 4775–4793.

Ferraro A J, Charlton-Perez A J & Highwood E J 2015 *Journal of Geophysical Research: Atmospheres* **120**, 414–429.

Ferraro A J, Highwood E J & Charlton-Perez A J 2011 *Geophysical Research Letters* **38**, L24706.

Ferraro A J, Highwood E J & Charlton-Perez A J 2014 *Environmental Research Letters* **9**(1), 014001.

Fyfe J C, Cole J N S, Arora V K & Scinocca J F 2013 *Geophysical Research Letters* **40**, 651–655.

Govindasamy B & Caldeira K 2000 *Geophysical Research Letters* **27**(14), 2141–2144.

Heckendorn P, Weisenstein D, Fueglistaler S, Luo B P, Rozanov E, Schraner M, Thomason L W & Peter T 2009 *Environmental Research Letters* **4**, 045108.

Iles C E & Hegerl G C 2014 *Environmental Research Letters* **9**(10), 104012.

Iles C E, Hegerl G C, Schurer A P & Zhang X 2013 *Journal of Geophysical Research Atmospheres* **118**(16), 8770–8786.

Kalidindi S, Bala G, Modak A & Caldeira K 2014 'Modeling of solar radiation management: a comparison of simulations using reduced solar constant and stratospheric sulphate aerosols'.

Keith D W, Parson E & Morgan M G 2010 *Nature* **463**(7280), 426–427.

Kleidon A & Renner M 2013 *Earth System Dynamics* **4**(2), 455–465.

Kvalevåg M M, Samset B H & Myhre G 2013 *Geophysical Research Letters* **40**(7), 1432–1438.

Lambert F H & Chiang J C H 2007 *Geophysical Research Letters* **34**, L13704.

Lambert F H & Webb M J 2008 *Geophysical Research Letters* **35**(16), 1–5.

Martin G M, Bellouin N, Collins W J, Culverwell I D, Halloran P R, Hardiman S C, Hinton T J, Jones C D, McDonald R E, McLaren A J, O'Connor F M, Roberts M J, Rodriguez J M, Woodward S, Best M J, Brooks M E, Brown a R, Butchart N, Dearden C, Derbyshire S H, Dharssi I, Doutriaux-Boucher M, Edwards J M, Falloon P D, Gedney N, Gray L J, Hewitt H T, Hobson M, Huddleston M R, Hughes J, Ineson S, Ingram W J, James P M, Johns T C, Johnson C E, Jones A, Jones C P, Joshi M M, Keen A B, Liddicoat S, Lock A P, Maidens A V, Manners J C, Milton S F, Rae J G L, Ridley J K, Sellar A, Senior C A, Totterdell I J, Verhoef A, Vidale P L & Wiltshire A 2011 *Geoscientific Model Development* **4**(3), 723–757.

McClellan J, Keith D W & Apt J 2012 *Environmental Research Letters* **7**(3), 034019.

Mitchell J F B, Wilson C A & Cunnington W M 1987 *Quarterly Journal of the Royal Meteorological Society* **113**(475), 293–322.

Moss R H, Edmonds J A, Hibbard K A, Manning M R, Rose S K, van Vuuren D P, Carter T R, Emori S, Kainuma M, Kram T, Meehl G A, Mitchell J F B, Nakicenovic N, Riahi K, Smith S J, Stouffer R J, Thomson A M, Weyant J P & Wilbanks T J 2010 *Nature* **463**(7282), 747–56.

Niemeier U, Schmidt H, Alterskjær K & Kristjánsson J E 2013 *Journal of Geophysical Research: Atmospheres* **118**.

Niemeier U, Schmidt H & Timmreck C 2011 *Atmospheric Science Letters* **12**(2), 189–194.

Niemeier U & Timmreck C 2015 *Atmospheric Chemistry and Physics* **15**(16), 9129–9141.

O'Gorman P A, Allan R P, Byrne M P & Previdi M 2012 *Surveys in Geophysics* **33**(3-4), 585–608.

Pendergrass A G & Hartmann D L 2014 *Journal of Climate* **27**(2), 757–768.

Pitari G, Aquila V, Kravitz B, Robock A, Watanabe S, Cionni I, Luca N D, Genova G D, Mancini E & Tilmes S 2014 *Journal of Geophysical Research: Atmospheres* **119**(5), 2629–2653.

Robock A, Marquardt A, Kravitz B & Stenchikov G 2009 *Geophysical Research Letters* **36**, L19703.

Schmidt H, Alterskjær K, Bou Karam D, Boucher O, Jones A, Kristjánsson J E, Niemeier U, Schulz M, Aaheim A, Benduhn F, Lawrence M & Timmreck C 2012 *Earth System Dynamics* **3**(2012), 63–78.

Stevens B, Giorgetta M, Esch M, Mauritsen T, Crueger T, Rast S, Salzmann M, Schmidt H, Bader J, Block K, Brokopf R, Fast I, Kinne S, Kornblueh L, Lohmann U, Pincus R, Reichler T & Roeckner E 2013 *Journal of Advances in Modeling Earth Systems* **5**(2), 146–172.

Thorpe L & Andrews T 2014 *Environmental Research Letters* **9**(6), 064024.

Tilmes S, Fasullo J, Lamarque J F, Marsh D R, Mills M, Alterskjær K, Muri H, Kristjánsson J E,

Boucher O, Schulz M, Cole J N S, Curry C L, Jones A, Haywood J, Irvine P J, Ji D, Moore J C, Karam D B, Kravitz B, Rasch P J, Singh B, Yoon J H, Niemeier U, Schmidt H, Robock A, Yang S & Watanabe S 2013 *Journal of Geophysical Research: Atmospheres* **118**(19), 11,036–11,058.

von Salzen K, Scinocca J F, McFarlane N a, Li J, Cole J N S, Plummer D, Verseghy D, Reader M C, Ma X, Lazare M & Solheim L 2013 *Atmosphere-Ocean* **51**(1), 104–125.

Weisenstein D K, Keith D W & Dykema J A 2015 *Atmospheric Chemistry and Physics* **15**(20), 11835–11859.

Wigley T M L 2006 *Science* **314**(5798), 452–454.